Choosing Optimal Wavelengths for Colour Laser Scanners

Lindsay W. MacDonald, 3D Imaging and Metrology Research Centre, Dept. of Geomatic Engineering, University College London

Abstract

Multiple sets of measured reflectance data were analysed to determine the combination of three laser wavelengths that would minimise the mean colorimetric difference between the laser illumination and D65. The optimum wavelengths for blue, green and red lasers were found to be in the ranges 450-460, 530-540 and 595-605 nm, close to Thornton's 'prime wavelengths of vision'. These optima were independent of both samples and colour difference metrics. The results were compared with the colorimetric performance of a commercial 3D colour laser scanner, in which the laser wavelengths are 473, 532 and 635 nm. It was found that two additional laser wavelengths would have to be added to the scanner to achieve a degree of colorimetric accuracy similar to the optimum three laser wavelengths. The effects on colour image rendering of the actual vs optimal wavelengths were demonstrated on a hyperspectral image.

Introduction

Colour laser scanners are well established as a means of capturing 3D representations of objects, especially in the cultural heritage field. At each point on the surface both the geometric coordinates (*x,y,z*) and the colour (*r,g,b*) can be accurately digitised. The Arius 3D laser scanner (Fig. 1) employs technology developed over the past 25 years at NRC, Canada [1]. The scan head is mounted on a massive Coordinate Measuring Machine (CMM) which provides fine control over positioning. In operation the laser beam is scanned by a galvanometer on the Y axis while the whole head assembly is moved along the X axis. At a given position of the head, the range of the scanner (in the Y-Z plane) is approximately 60x60 mm. Laser spot size is nominally 80 µm and the surface is sampled at 100 µm internals in normal scanning mode and at 50 µm in fine mode. The positioning accuracy of the CMM is 25 µm. The scanner at UCL has been used effectively for digitising museum collections for e-Science applications [2].

Figure 1. *The Arius 3D colour laser scanner at UCL*

Colour laser scanners pose a colorimetric challenge for the digitisation of reflective objects because, unlike the human visual system and digital cameras with broadband sensitivity, they sample the spectrum at single wavelengths. More properly, they illuminate the sample at one or more monochromatic wavelengths, and sense the intensity of the reflected light. For a colour scanner with red, green and blue lasers the RGB triplet at each pixel position depends only on the wavelength of each laser and the surface reflectance of the object at those three specific wavelengths (assuming a Lambertian surface and linearity of the detector). Although this arrangement is highly metameric, it produces acceptable results for a range of media because natural reflectance spectra are broadband and can be sampled with sufficient accuracy at a few widely-spaced wavelengths. The question then arises as to which three wavelengths would be optimum for trichromatic imaging of typical colorants?

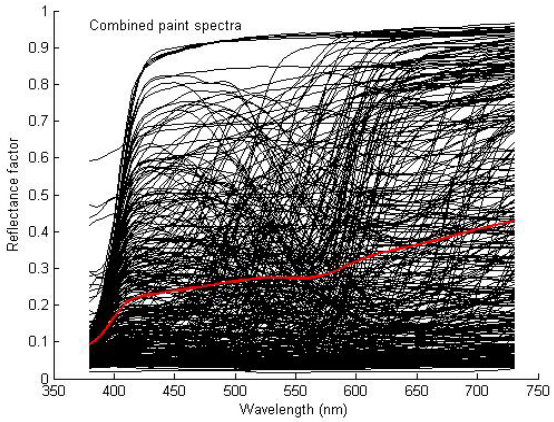

Figure 2. *Measured reflectance spectra of 334 paint samples and mean (red);*

Method

For an initial assessment, three independent sets of colour reflectance spectra were obtained, all measured from physical paint samples. Each dataset was interpolated to intervals of 5 nm over the range 380-730 nm (a vector of 71 reflectance factors), then combined into a single dataset containing 334 spectra (Fig. 2):

- GretagMacbeth DC Chart – 170 patches (no gloss)
  – measured at 10 nm intervals with *i1Pro;*
- Berns-Taplin RIT pigment set – 100 patches
  – measured at 10 nm intervals with *i1Pro;*
- National Gallery pigment set – 64 patches
  – measured at 2 nm intervals with M*onolight.*

The three lasers in ensemble can be regarded as a tri-band white light illuminating the surface of the object [3]. Tristimulus values *X,Y,Z* were calculated for each reflectance sample in a dataset under D65 and under multi-laser illumination, using the Judd-Vos modification of the CIE 2-degree Standard Observer [4]. These

were converted to CIELAB values using the respective spectra of D65 and equal unit power of the lasers as reference white, and the colour difference ΔE^*_{ab} was calculated. The median and mean of the colour differences were calculated over all the samples in the dataset. By exhaustive search, the combination of laser wavelengths at 5 nm intervals was found that minimised the mean colour difference between D65 and three-laser illumination over the pigment set. The search space was limited to all combinations of laser wavelengths, at 5 nm intervals, in the three broad ranges: blue 380-495 nm; green 500-570 nm; and red 575-730 nm.

For a proper basis for comparison of colour differences, the relative power of the three laser sources was adjusted to have the same tristimulus values as the standard D65 illuminant, i.e. X=94.33, Y=100, Z=104.155. Note that because the Judd-Vos tristimulus functions were employed [4], the tristimulus values for D65 were different from the customary X=95.04, Y=100, Z=108.89 associated with the CIE 1931 2-degree standard observer.

The conversion from laser intensity values L_r, L_g, L_b to tristimulus values X, Y, Z is simplified from the usual summation because the laser spectra can be regarded as delta functions, with a non-zero value at a single wavelength. (In this study the use of colorimetric data at 5nm wavelength intervals led to the rounding of the laser wavelengths to the nearest multiple of 5 nm, namely 475, 530, 635 nm.) Each tristimulus value is then simply the sum of the tristimulus function at each of the three laser wavelengths, weighted by the laser intensity:

$$\begin{bmatrix} X \\ Y \\ Z \end{bmatrix} = K \begin{bmatrix} \overline{x_r} & \overline{x_g} & \overline{x_b} \\ \overline{y_r} & \overline{y_g} & \overline{y_b} \\ \overline{z_r} & \overline{z_g} & \overline{z_b} \end{bmatrix} \begin{bmatrix} L_r \\ L_g \\ L_b \end{bmatrix} \quad \text{i.e. } \mathbf{T} = K\mathbf{ML} \tag{1}$$

where $K = \frac{100}{\overline{y_r}L_r + \overline{y_g}L_g + \overline{y_b}L_b}$ is a normalising factor to make Y=100, and $\overline{x_r}$, $\overline{y_r}$, $\overline{z_r}$ = values of the $\bar{x}, \bar{y}, \bar{z}$ tristimulus functions at the red laser wavelength, and similarly for the green and blue lasers. For the Judd-Vos observer at the approximated Arius laser wavelengths of 475,530, 635 nm, the values of the coefficients are:

$$\mathbf{M} = \begin{bmatrix} 0.5340 & 0.1908 & 0.1501 \\ 0.2170 & 0.8849 & 0.1037 \\ 0.0001 & 0.0363 & 1.0125 \end{bmatrix} \tag{2}$$

Eq. (1) can be inverted to express the laser intensities as a function of tristimulus values:

$$K\mathbf{L} = \mathbf{M}^{-1}\mathbf{T} \tag{3}$$

where the inverse matrix is:

$$\mathbf{M}^{-1} = \begin{bmatrix} 2.0478 & -0.4310 & -0.2594 \\ -0.5043 & 1.2410 & -0.0524 \\ 0.0179 & -0.0444 & 0.9896 \end{bmatrix} \tag{4}$$

The power of the three lasers can be varied to change the white balance. We seek to set the laser intensity values so that the tristimulus values of white are equal to those of the D65 illuminant. Then, setting K=1, we have:

$$\mathbf{L}_W = \mathbf{M}^{-1}\mathbf{T}_w = \mathbf{M}^{-1} \begin{bmatrix} 94.33 \\ 100 \\ 104.155 \end{bmatrix} = \begin{bmatrix} 123.05 \\ 71.08 \\ 100.32 \end{bmatrix} = 71.08 \begin{bmatrix} 1.73 \\ 1.00 \\ 1.41 \end{bmatrix} \tag{5}$$

By using the equations above, the relative laser power was adjusted to give a white balance corresponding to D65 for each combination of the changing wavelengths of the red, green and blue lasers during the search procedure.

Optimum Wavelengths

The three curves in Fig. 3 represent one-dimensional sections through the three-dimensional distribution of mean ΔE^*_{ab} values for the combined dataset. The global minimum point was well defined with respect to all three variable laser wavelengths, and both mean and median measures of error distributions gave the same result. The optimum wavelengths were 460, 535 and 600 nm.

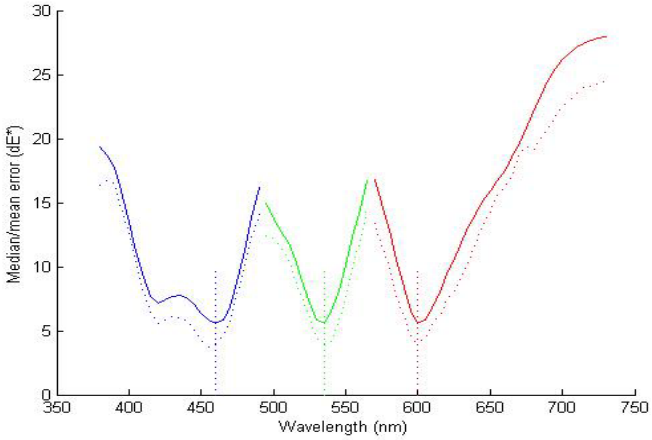

Figure 3. *Mean (solid line) and median (dotted line) values of ΔE^*_{ab} colour difference for 334 paint spectra.*

The results were similar for all three datasets when evaluated individually (Table 1). The mean error at the optimum wavelength triplet was consistently in range 5-6 ΔE^*_{ab} and median 3-4 ΔE^*_{ab}.

Table 1. Optimum laser wavelengths and error values.

Chart	#	Optimum (nm)	Med	Mean	Max
NG pigments	64	460, 535, 600	4.02	6.01	21.50
Berns-Taplin acrylic data	100	465, 540, 605	3.53	5.34	21.46
GM DC Chart	170	460, 530, 595	3.12	5.28	46.40
Combined dataset	334	460, 535, 600	3.99	5.60	34.15

The optimum results were compared with the colorimetric performance of the Arius 3D colour laser scanner, in which the laser wavelengths are 473, 532 and 635 nm. The mean error of the scanner for the patches in the combined dataset is 3.4 times greater than for the optimum (Table 2). The maximum error for the optimum wavelengths was produced by colour patch 21, a strong red, which has maximum slope in the reflectance spectrum between 600 and 620 nm. The maximum error for the scanner wavelengths was produced by colour patch 284, a strong yellow, with maximum slope in reflectance between 545 and 565 nm.

Table 2. Error values for colour laser scanner

Chart	Samples	Median	Mean	Max
National Gallery chart	64	21.54	23.84	80.49
Berns-Taplin acrylic	100	13.64	16.83	66.29
GM DC chart	170	15.09	18.16	63.43
Combined dataset	344	15.31	19.02	80.84

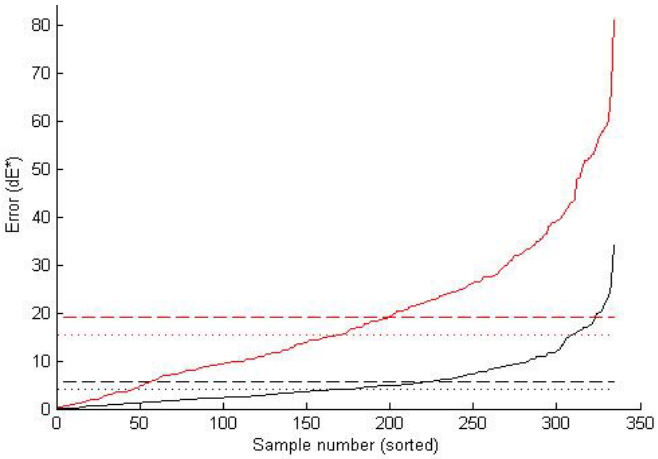

Figure 4. *Colour difference ΔE^*_{ab} values for each of 334 spectra, sorted into ascending order, with median (dotted line) and mean (dashed line). The black line (lower) shows the errors for optimum laser wavelengths and the red line (upper) shows the errors for approximate scanner wavelengths.*

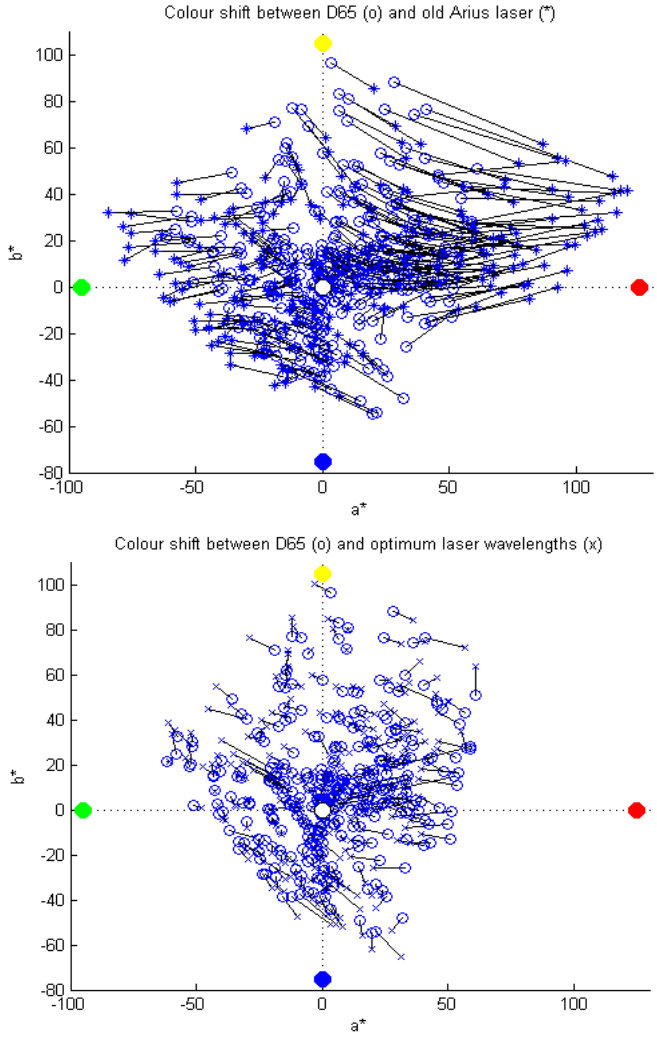

Figure 5. *Error vectors in the CIELAB a*-b* plane between samples of the combined art pigment dataset under D65 and: (top) actual scanner laser wavelengths; (bottom) optimal laser wavelengths.*

The difference in colorimetric accuracy between the scanner and the optimum laser wavelengths can be seen clearly in Fig. 4, where the error values have been sorted into ascending order. The 90th percentile error for the optimum wavelengths was less than the mean error for the actual scanner. A similar disparity can be seen by plotting the error vectors between the *a*-b** coordinates of each sample under D65 and its corresponding coordinates under the laser illumination (Fig. 5). For the scanner wavelengths there is a large displacement of colours in the hue range from magenta to orange towards red (+*a**) and a lesser displacement of greens and blues towards green (–*a**). For the optimum laser wavelengths the displacements are much smaller and their directions rather random

Evaluation with other Reflectance Datasets

A set of 899 measured spectra of synthetic dyes on polyester fabric samples in the Chinese Natural Color System (CNCS) was tested. These occupy a large volume of colour space. The optimum sampling wavelengths were 460, 535 and 605 nm (Fig. 6), with the minima for the green and red lasers being well defined.

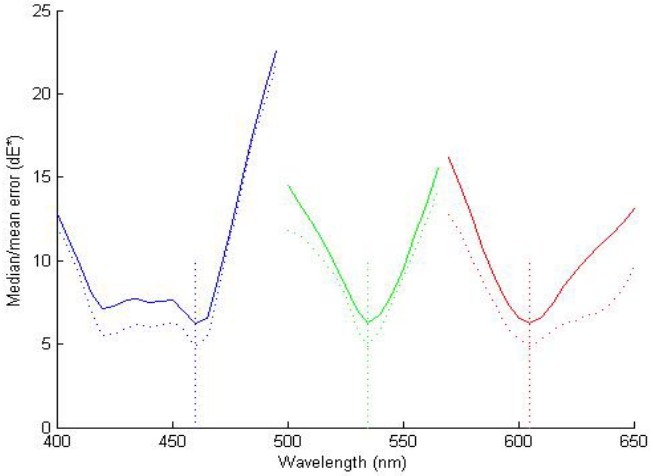

Figure 6*. Mean (solid line) and median (dotted line) values of colour differences ΔE^*_{ab} for 899 textile samples in the Chinese CNCS atlas.*

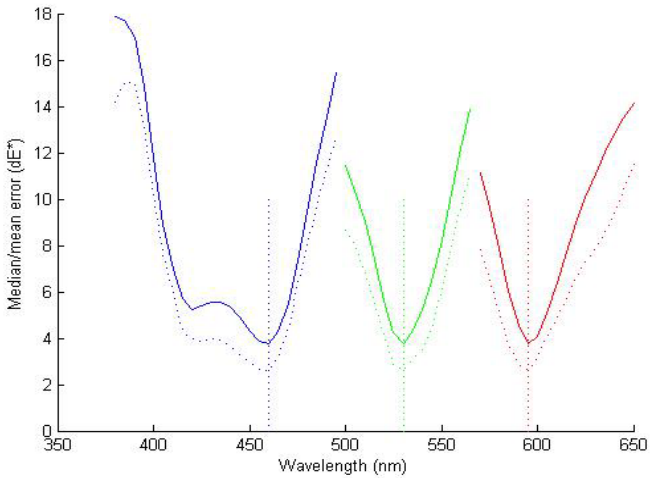

Figure 7. *Mean (solid line) and median (dotted line) values of colour differences ΔE^*_{ab} for 1600 glossy samples in the Munsell atlas.*

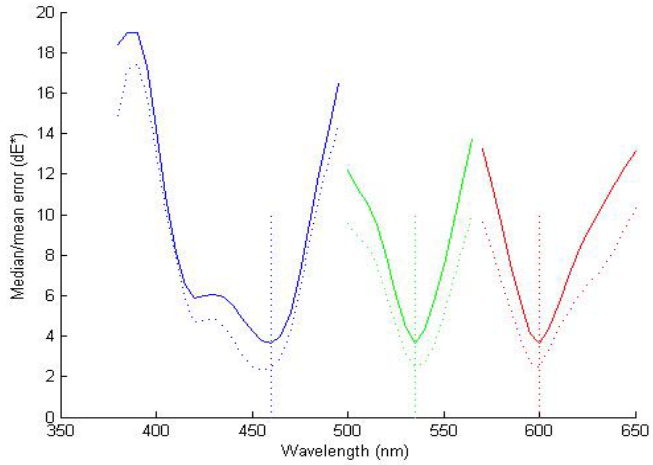

Figure 8. *Mean (solid line) and median (dotted line) values of colour differences for1950 matte samples in the Swedish NCS atlas, using the CIELAB ΔE^*_{ab} metric.*

A set of 1600 measured spectra of samples in the Munsell gloss atlas was tested. The original 1nm data was abridged to 5nm intervals. These occupy a large volume of colour space and sample the space quite uniformly. The optimum sampling wavelengths were 460, 530, 595 nm (Fig. 7), with the minima for the green and red lasers being well defined. The minima for blue were broader across the range 420-460 nm. The procedure was repeated for the Munsell gloss atlas, using the full 1nm reflectance dataset over the range 380-780 nm. The 1nm datasets were also used for the D65 illuminant and the CIE 1931 Standard Observer, both taken from the CVRL database. The results showed well-defined minima at optimum wavelengths of 461, 529, 597 nm.

A set of 1950 measured spectra of the Swedish Natural Color System (NCS) atlas was tested. These occupy a large volume of colour space and sample the space quite densely, especially for pastels. The optimum sampling wavelengths were 460, 535 and 600 nm (Fig. 8), with the minima for the green and red lasers being well defined. The minima for blue were broader across the range 420-460 nm because of the form of the Judd-Vos observer.

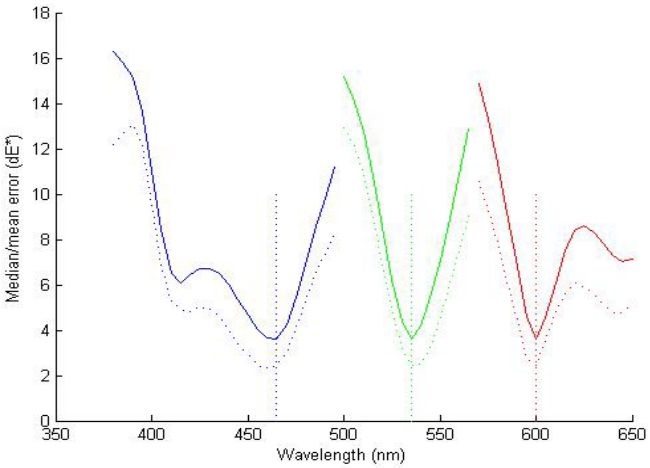

Figure 8. *Mean (solid line) and median (dotted line) values of colour differences for1950 matte samples in the Swedish NCS atlas, calculating RMS differences of J,a,b in the CIECAM02 colour appearance space.*

The influence of the choice of colour space on the error minimisation procedure was investigated for the Swedish NCS dataset. All the uniform colour spaces gave broadly similar results for the optimum wavelengths, although the behaviour of the minima for the blue laser wavelength varied. CIECAM02 gave more sharply defined peaks for red and green (Fig. 9) than did CIELAB (Fig. 8). The XYZ metric gave smaller minimum error values because it is linear in light intensity, and so de-emphasises dark colours relative to the lightness as a cube root of intensity in the UCS metrics.

Discussion

The optimum three laser wavelengths identified in this study of 450-460, 530-535 and 590-600 nm are very close to the 'prime colors' of approximately 450, 530 and 610 nm identified in 1971 by Thornton [5] as the wavelengths of peak visual sensitivity. Thornton later refined the specifications for the prime wavelengths of the average human, CIE 2°, and CIE 10° observers respectively to: Blue 450, 447, 446 nm; Green 533, 541, 538 nm; Red 611, 604, 600 nm [6]. He showed that for 'white' light made up of three monochromatic wavelengths, the colour rendering index (CRI) could be optimised by choosing the three prime wavelengths (Fig. 10). He demonstrated this empirically by holding constant two of the wavelengths in the set 450, 540, 610 nm and varying the third and calculating the CRI for each combination. Repeating the calculations for various power ratios of the three sources, to achieve various correlated colour temperatures, always gave the same result.

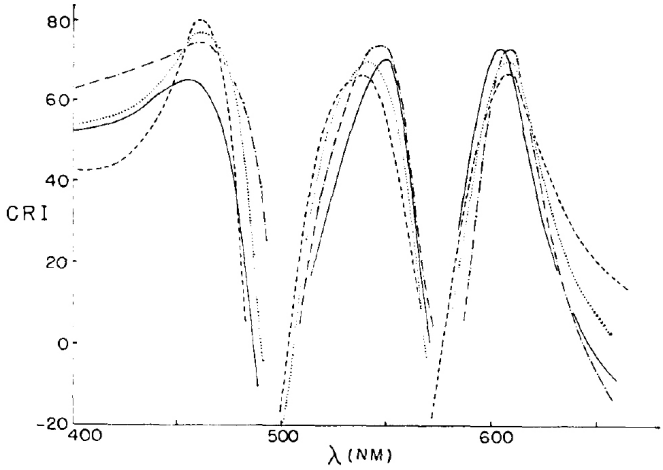

Figure 10. *CRI of white light comprising three spectral colours, from Thornton (1971).*

Thornton also showed that other wavelengths, which he termed 'anti-prime', gave disastrous results, namely wavelengths near 495, 575 and beyond 640 nm. He concluded that "… the [optimum] three-line SPD is superior to that of the commercial fluorescent lamp of the same color in both luminosity and CRI, notwithstanding the common opinion that discontinuous distributions cannot provide good color rendering", and further "it is apparently a more efficient use of power to sample the reflectance spectrum of an object at these three unique wavelengths than to waste power by reflection from the object in the insensitive regions near 500 nm, 580 nm and in the deep violet and deep red."

In another study [7], Thornton showed that the prime wavelengths are particularly effective in altering the perceived chromaticity of a light source or illuminated object. Plotting the normalised ratio $(P_i + P_j)/P_\lambda$ of power in two monochromatic colours i, j of fixed wavelengths relative to a variable third wavelength λ from 450, 540 and 610 nm, he showed how the efficacy falls away from the optimum as any of the lights moves away from the corresponding prime wavelength. In effect the curves may be considered as the visual response (or luminosity) per watt as a function of wavelength, i.e. the inverse of visual sensitivity. Thornton summarised that: "The chromaticity of an element in any visual scene is established with minimum power input to the eye when light from that element is composed of spectral colors near the prime wavelengths."

Thornton subsequently showed that the three prime wavelengths are those at which unit-power monochromatic lights induce the largest tristimulus gamut (in terms of the volume of the parallelepiped spanned by the tristimulus vectors of these lights) and are therefore optimal as the dominant wavelengths of the primaries for displays [8]. They are also the wavelengths at which natural metameric reflectance spectra tend to cross each other [9].

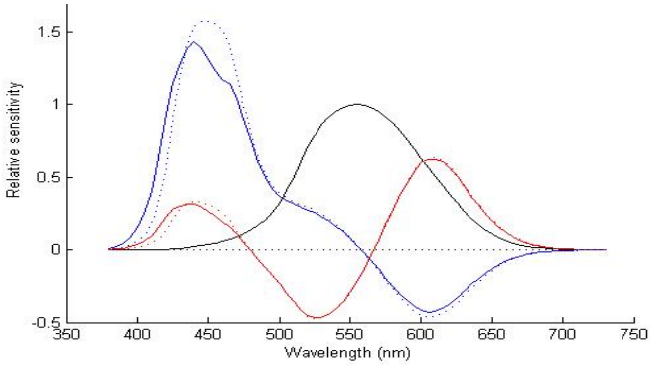

Figure 11. *Y tristimulus function and two orthonormal vectors for Judd-Vos observer (dotted lines) and CIE Standard 2-deg observer (solid lines).*

It is instructive to separate the tristimulus functions is Gram-Schmidt orthonormalisation, starting with the luminance function $\bar{y}$ as the first basis vector and then projecting the $\bar{x}$ and $\bar{z}$ functions onto it:

$$U_1 = \bar{y}\,, \quad U_2 = \bar{x} - \frac{\bar{x}\cdot\bar{y}}{\bar{y}\cdot\bar{y}}\,\bar{y}\,, \quad U_3 = \bar{z} - \frac{\bar{z}\cdot\bar{y}}{\bar{y}\cdot\bar{y}}\,\bar{y} - \frac{\bar{z}\cdot\bar{x}}{\bar{x}\cdot\bar{x}}\,\bar{x} \qquad (6)$$

The resulting orthogonal functions (Fig. 11), which correspond closely to the decorrelated luminance and opponent chrominance signals in the neural visual pathway, have an obvious magenta-green and blue-yellow formation. The relationship between the orthonormal functions U_1, U_2, U_3 and the tristimulus functions $\bar{x}$, $\bar{y}$, $\bar{z}$ is:

$$\begin{bmatrix} U_1 \\ U_2 \\ U_3 \end{bmatrix} = \begin{bmatrix} 1 & 0 & 0 \\ -a_{21} & 1 & 0 \\ -a_{31} & -a_{32} & 1 \end{bmatrix} \begin{bmatrix} \bar{y} \\ \bar{x} \\ \bar{z} \end{bmatrix} = \begin{bmatrix} 1 & 0 & 0 \\ -0.7337 & 1 & 0 \\ -0.1114 & -0.5770 & 1 \end{bmatrix} \begin{bmatrix} \bar{y} \\ \bar{x} \\ \bar{z} \end{bmatrix} \qquad (7)$$

For the CIE standard observer the maxima of the second and third orthonormal functions are at 610 and 450 nm, and the minima are at 525 and 605 nm. For the Judd-Vos observer the maxima are shifted to 605 and 440 nm. From this it is clear that the significance of the prime wavelengths is that they produce maximal excitation of the opponent channels, and hence the greatest chromatic response from the human visual system. At the anti-prime wavelength of 565 nm the two orthonormal functions cross one another close to zero, and so this wavelength has the least ability to produce a chromatic response.

Buchsbaum and Gottschalk applied principal component analysis to the Vos-Walraven cone sensitivity functions, to derive an achromatic and two opponent chromatic channels [10]. They showed that such channels provide an efficient transmission of information in the visual pathway, and thus could reconcile the Young-Helmholtz trichromatic receptor theories of vision with the Hering and Hurvich-Jameson opponency theories [11]. The maxima and minima of opponent channels lie at 440, 530, 610 nm, exactly the prime wavelengths identified by Thornton (Fig. 12).

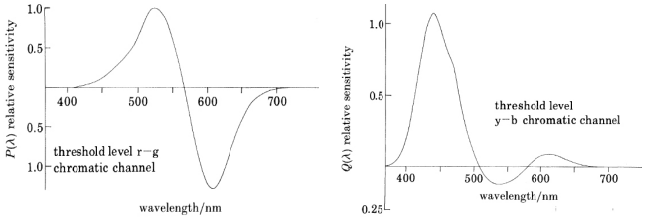

Figure 12. *Second and third principal components of the Vos-Walraven photoreceptor sensitivity functions, from Buchsbaum and Gottschalk (1983).*

Colour Rendering

The improved visual efficiency of the optimal laser wavelengths can be seen in the CIE general colour rendering index (CRI), which increases from 48.6 for the approximate scanner wavelengths of 475, 530, 635 nm to 75.4 for the optimal laser wavelengths of 460, 535, 600 nm. This is largely due to the reduced shift of colorimetric values toward red (Fig. 13 right).

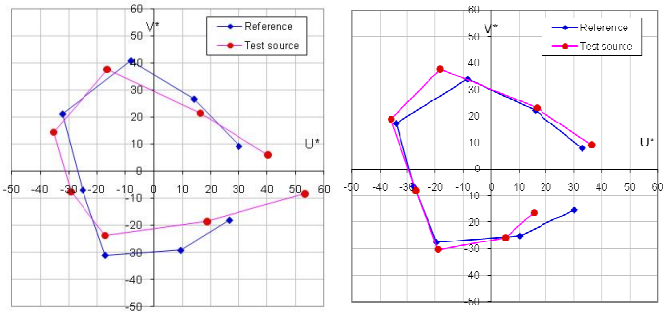

Figure 13. *Colour rendering of the eight CIE test colours: (left) under the Arius scanner wavelengths; (right) under the optimal laser wavelengths;*

To demonstrate the visual effect of the choice of laser wavelengths, synthetic images were produced for the Macbeth ColorChecker chart (Fig. 14). The tristimulus values were calculated for the measured reflectance spectrum of each patch under the corresponding light source (D65 or triple laser), then converted to L^*,a^*,b^* using the light's tristimulus values as the reference white. Colours were checked to ensure that they lay within the colour gamut of sRGB, mapped onto the gamut boundary if necessary, then converted back to X,Y,Z using D65 reference white, thence to 8-bit RGB signals for an sRGB display.

The colours of the chart under the optimum laser wavelengths give a generally acceptable visual match to the colours under D65, except notably for the red patch which is greatly desaturated because its reflectance rises sharply between 600 and 620 nm, and the laser at 600 nm falls just too short. The colours of the chart under the wavelengths of the Arius 3D laser scanner, however, are grossly over-saturated, especially magenta, red, pink, orange and lime. Even the 'light skin' is far too pink.

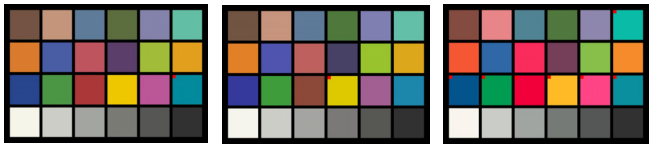

Figure 14. *Synthetic images of the Macbeth ColorChecker Chart for (left) D65 illumination; (centre) optimum laser wavelengths; (right) the wavelengths of the Arius 3D colour laser scanner. The red spots indicate colours that were outside the sRGB gamut.*

A test image was selected from the hyperspectral set produced by Foster and Nascimento [12]. The image was originally acquired with a monochrome digital camera with a tunable birefringent filter mounted in front of the lens. The image size was 820x820 pixels, representing the normalised scene radiance at each point in 31 spectral bands from 400 to 700 nm at 10nm intervals.

The image spectral data was interpolated to 5nm intervals, giving a vector of 61 values for each pixel, then rendered with the Judd-Vos observer and the three illumination sources (D65 and the triple laser combinations for optimum and Arius scanner) to give the sRGB images in Fig. 15. In each case the power of the three lasers was adjusted to give the same *X,Y,Z* tristimulus values as D65 white. Neither of the laser images is a good match to the D65 image, but the image from the optimum laser wavelengths has the better overall colour balance apart from some loss of saturation in the reds. The laser scanner, however, exhibits a red cast in yellow and orange and in the brown wall tiles in the background and the basketball in the foreground. It grossly distorts the red areas and over-saturates the green areas.

Figure 15. *Hyperspectral image rendered for: (left) D65 illumination; (centre) optimum laser wavelengths; (right) Arius 3D colour laser scanner.*

Conclusion

This study has confirmed the significance of the prime wavelengths of vision as the optimal wavelengths for three monochromatic lasers in a 3D colour scanner. The existing green laser at 532 nm in the Arius scanner is close to the optimum, but the wavelengths of both the red and blue lasers are too long, causing substantial colorimetric distortion and poor colour rendering of objects. This creates significant problems for the veridical colour capture of objects in museum collections.

If the Arius scanner with its current laser wavelengths could be augmented with one additional laser, to sample the surface at four discrete wavelengths, what would be the optimum wavelength of this fourth laser? Applying the same method to calculate the mean colour difference over the combined set of art pigments for each possible wavelength of the four lasers showed that the optimum wavelength would be 575 nm and the mean error would be reduced to less than 8 ΔE^*_{ab}. Where the three RGB lasers were fixed and one was allowed to vary, the variation in mean error was less marked than when all four laser wavelengths could vary. Similarly, adding a fifth laser at an optimum wavelength of 415 nm would reduce the mean error to less than 3 ΔE^*_{ab}. A sixth laser would produce little improvement. Thus by choosing three optimal laser wavelengths the colorimetric performance would be almost as good as if two additional lasers of intermediate wavelengths were added to the existing three lasers of the Arius scanner.

References

[1] J. Taylor, J.-A. Beraldin, G. Godin, L. Cournoyer, R. Baribeau, F. Blais, M. Rioux and J. Domey, NRC 3D Technology for Museum and Heritage Applications *J. Visualization and Computer Animation*, 14(3):121-138 (2003).

[2] M. Hess, F. Simon Millar, Y.-H. Ong, S. Robson, G. Were, I. Brown and S. MacDonald, 3D Colour Scans For Object Assessment, *Proc. Electronic Visualisation and the Arts (EVA) Conf.*, London (2008).

[3] R. Baribeau, M. Rioux and G. Godin, Color Reflectance Modeling using a Polychromatic Laser Range Sensor, *IEEE Trans. Patt. Anal. and Machine Intelligence*, 14(2):263-269 (1992).

[4] J.J. Vos, Colorimetric and photometric properties of a 2-deg fundamental observer. *Color Research and Application*, 3:125-128 (1978). Judd-Vos CMFs were downloaded from http://www.cvrl.org/

[5] W.A. Thornton, Luminosity and color-rendering capability of white light. *J. Opt. Soc. Amer.,* 61:191-194 (1971).

[6] W.A. Thornton, Spectral sensitivities of the normal human visual system, color matching functions and their principles, and how and why the two sets should coincide, *Color Research and Application*, 24:139 –156 (1999).

[7] W.A. Thornton, Three-color visual response, *J. Opt. Soc. Amer.*, 62:457-459 (1972).

[8] W.A. Thornton, Suggested Optimum Primaries and Gamut in Color Imaging, *Color Research and Application*, 25(2):148-150 (2000).

[9] M.H. Brill, G.D. Finlayson, P.M. Hubel and W.A. Thornton, Prime Colours and Colour Imaging, *Proc. 6th IS&T/SID Color Imaging Conf.*, 33-42 (1998).

[10] G. Buchsbaum and A. Gottschalk, Trichromacy, opponent colours coding and optimum colour information transmission in the retina, *Proc. Royal Society B (London)*, 220:89-113 (1983).

[11] L.M. Hurvich and D. Jameson, Some Quantitative Aspects of an Opponent-Colors Theory. II. Brightness, Saturation, and Hue in Normal and Dichromatic Vision, *Vis. Res.* 45(8):602-616 (1955).

[12] S.M.C. Nascimento, F.P. Ferreira and D.H. Foster, Statistics of spatial cone-excitation ratios in natural scenes, *J. Opt. Soc. Am. A,* 19(8):1484-90 (2002).

Author Biography

Lindsay MacDonald is a Fellow of IS&T and has had twin careers in industrial R&D and academia as a colour engineer. He has edited eight books on colour image science and its applications in cultural heritage. He is a Consultant Editor for the IS&T book series on image science published by John Wiley. He was Co-Chair of the Color Imaging Conference in 1998 and is currently a member of the Executive Committee of the International Colour Association (AIC) and Editor of the annual AIC Newsletter.